Int. J. Environ. Res., 10(2):273-290, Spring 2016
ISSN: 1735-6865

Eutrophication Modeling Using Variable Chlorophyll Approach

Abdolabadi, H.*, Sarang, A., Ardestani, M., and Mahjoobi, E.

Graduate Faculty of Environment, University of Tehran, Tehran, Iran

Received 5 July 2015; Revised 22 Dec. 2016; Accepted 26 Dec. 2016

ABSTRACT: In this study, eutrophication was investigated in Lake Ontario to identify the interactions among effective drivers. The complexity of such phenomenon was modeled using a system dynamics approach based on a consideration of constant and variable stoichiometric ratios. The system dynamics approach is a powerful tool for developing object-oriented models to simulate complex phenomena that involve feedback effects. Utilizing stoichiometric ratios is a method for converting the concentrations of state variables. During the physical segmentation of the model, Lake Ontario was divided into two layers, i.e., the epilimnion and hypolimnion, and differential equations were developed for each layer. The model structure included 16 state variables related to phytoplankton, herbivorous zooplankton, carnivorous zooplankton, ammonium, nitrate, dissolved phosphorus, and particulate and dissolved carbon in the epilimnion and hypolimnion during a time horizon of one year. The results of several tests to verify the model, close to 1 Nash-Sutcliff coefficient (0.98), the data correlation coefficient (0.98), and lower standard errors (0.96), have indicated well-suited model's efficiency. The results revealed that there were significant differences in the concentrations of the state variables in constant and variable stoichiometry simulations. Consequently, the consideration of variable stoichiometric ratios in algae and nutrient concentration simulations may be applied in future modeling studies to enhance the accuracy of the results and reduce the likelihood of inefficient control policies.

Key words: Constant and variable stoichiometry, Eutrophication, Lake Ontario, System dynamics

INTRODUCTION

Eutrophication is a complex natural process, which occurs gradually and affects the quality of water ýbodies. It is one of the most common problems affecting the quality management of lakes (Andersen et al., 2002; Chapra, 1997; Jong et al., 2002).ý However, rapid population growth, increased energy consumption, and a range of human activitieshas acceleratedd the nutrient enrichment of aquatic systems Glibert et al., 2011). The increased nutrient concentrations can lead to the overgrowth of aquatic plants and algal bloom, which have adverse environmental, economic, and social effects (Glibert et al., 2010; Nixon, 1995). The undesirable effects of these phenomena include the algal bloom and its toxic effects, shading of the lake surface, the prevention of light penetration into deep water, oxygen depletion due to the decomposition and respiration of the biomass, and aquatic death (Anderson et al., 2006; Glibert et al., 2005). Depending on their effects on water bodies and the ecosystems in a region (such as changes in the populations in ecosystems), certain ýphenomena should be given serious consideration by modelers, managers, and planners (Grégoire & Soetaert, 2010; Van England, 2010).

Systematic thinking using simulation tools is considered to be a new approach for preventing and mitigating water quality problems. Modeling complex processes and phenomena can facilitate a more precise understanding of phenomena and their relationships to various parameters (Ford, 1999). Simulation and prediction models can also be considered as bridges between research and management, which may help to understand the relationships between variables and the advanced management of scenarios to prevent and control undesirable effects (Holling, 1978). Another important issue that needs to be addressed is the time scale of modeling and simulations, which can be short term (daily and seasonal) or long term (annual or decades). Short-term simulation models can provide warning alerts for local agencies, which may facilitate the appropriate preparation and decision making required to address specific problems and

*Corresponding author E-mail: h.abdolabadi@ut.ac.ir

control their outcomes (Glibert et al., 2010; Ishizak et al., 2006).

Many models have been developed to simulate the concentrations of nutrients, algae, zooplankton, etc., and the complexity of these models has been determined by the requirements of the model and the availability of data (Grégoire & Friedrich, 2004; Grégoire et al., 2008). Many studies have investigated lake and reservoir parameters, such as thermal stratification, nutrient concentrations, primary production, algal bloom, and dissolved oxygen depletion (O'Brien, 1974). However, the focus of most models has been the impact of nutrient limitation (especially phosphorus), light limitation, and zooplankton grazing on the phytoplankton growth (Flynn et al., 2008; Kuo et al., 2004; Kuo et al., 2007ý). Current numerical models assess the interactions between the variables involved with eutrophication entirely in terms of their physiological, chemical, and hydrodynamic parameters (Davidson et al., 2012; Glibert et al., 2011; Li et al., 2012; Mitra & Flyn, 2010; O'Neil et al., 2011; Özkundakci et al., 2011; Wang et al., 2012). In recent years, the turbidity of water bodies has been reduced due to the development of wastewater purification and pollutant control approaches (Chapra, 1997). Therefore, fluctuations in the light penetration into the water column, as well as nutrient limitations and their effects on nutrient levels in algae cells, have affected the growth rate of cells due to the internal stoichiometry of nutrients, which are particularly important to modelers using variable stoichiometry (Bowie et al., 1985; Flynn, 2005a, 2005b, 2010). It should also be noted that the possibility of temporal changes in extreme conditions and the probability of failure of applied control strategies are increased by changes in the algal growth rate. Thus, the application of models that can assess and describe complex behavioral changes using simple and intelligible structures will facilitate more precise evaluations and reliable decision making to control these phenomena (Afshar et al., 2011).

The goals of this study were as follows. a) To develop a lake eutrophication simulation model comprising nutrient food chains, the prey, and predators, and their interactions using a system dynamics approach. b) To investigate the different quality parameter concentrations in simulations of algae concentrations using constant and variable stoichiometry. c) To develop a training-based model that reflected concepts and intricate relationships in interpretive frameworks to support decision-makers. The system dynamics approach was adopted to analyze the eutrophication process on a short time scale and to study the causal loops of its parameters.

MATERIALS & METHODS

Systems modeling can support the simulation, analysis, and evaluation of policies. A comprehensive and systematic view is essential because of the interactions and dependencies between the components of complex systems, while it also facilitates effective training and management. Object-oriented models based on system dynamics concepts are comprehensive approaches that can simulate the behavior and structure of the components of a complex system (Sterman, 2000). The system dynamics approach has been used previously to simulate several issues related to the quality and quantity management of water resources (Ahmad & Simonovic, 2004, 2006; Gelda & Effler, 2007; Ruley & Rusch, 2004; Simonovic, 2000, 2009; Simonovic & Fahmy, 1999; Tidwell et al., 2004; Vezjak et al., 1998).

In this study, the system dynamics methodology was used to simulate the eutrophication process because it is a powerful and simple high complexity approach (Elshorbagy & Ormsbee, 2006). The system dynamics approach is based on feedback relationships among variables and the feedback systems are affected by their past behavior (Forrester, 2007). These systems contain closed-loop structure where the results of past activities can affect future behavior. System dynamics models simulate the behavior of complex systems over time (Sterman, 2000). In these models, an initial causal loop diagram of the desired problem is drawn and a graphical diagram of the model is then plotted using the stock components, flow, arrows, and converters (Ford, 1999). The causal loop diagram of the eutrophication model consisted of reinforcing and balancing loops. The combination of positive and negative feedback loops allow the system to reach equilibrium. Fig. 1 shows the causal loop diagram of the main state variables in the system and their feedback loops. For instance, the feedback amongst some main variables can be described as:

As the phytoplankton concentration increases, the concentration of herbivorous zooplankton will enhance owing to grazing process as well as the concentration of carnivorous zooplankton. As a result, the grazing rate rises and the growth of phytoplankton will be regulated by zooplankton concentration (Balance loop). Furthermore, augmenting the phytoplankton concentration leads to less nutrients concentration and reduction of nutrients concentration hampers the growth of phytoplankton (Balance loop). On the other hand, decomposing of phytoplankton heightens the concentration of carbon pool. Additionally, if carbon

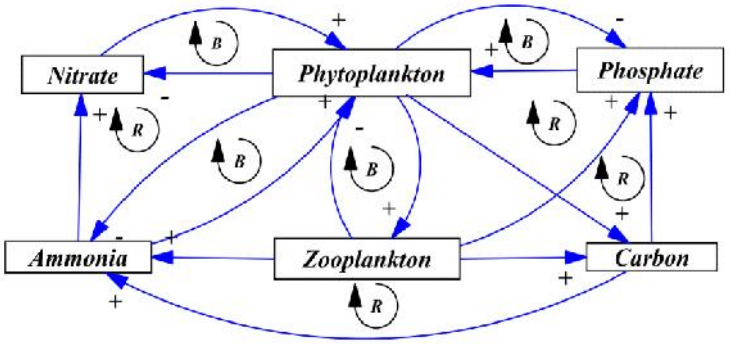

Fig. 1. Causal loop diagram of the eutrophication model

concentration is on the increase, the nutrient concentration will boost and eventually the phytoplankton concentration will foster (Reinforce loop). All of the paramount parameters, their relationships, and their impacts on the state variables were determined and the structure of the model was produced for each state variable based on its control equations.

In this study, the vital parameters that affected eutrophication were phytoplankton, herbivorous and carnivorous zooplankton, ammonium, nitrate, soluble phosphorus, and dissolved and particulate carbon. These parameters were considered in the simulation as 16 state variables in the epilimnion and hypolimnion. Table 1 presents these state variables and their description and initial values. To demonstrate the utility of the model, a simulation model was conducted in Lake Ontario over one year (short time scale). The eutrophication model was based on seasonal temperature changes because stratification of the lake divided it into the epilimnion and hypolimnion, each of which was considered to be completely mixed. These two parts were connected by diffusion and the inputs and outputs of the lake via the epilimnion. Lake Ontario is one of the five Great Lakes of North America and it is the 14th largest lake in the world. It is bounded on the north and southwest by the Canadian province of Ontario and on the south by the American state of New York. The Great Lakes watershed is a region of high biodiversity and Lake Ontario is important because of its diversity of birds, fish, reptiles, amphibians, and plants. The lake's primary source is the Niagara River, which drains Lake Erie, while the St Lawrence River serves as the outlet. The drainage basin covers 64,030 km^2 and 49% of this drainage basin is forested, 39% is agricultural, while the remaining 13% is urban (Agency USEPA, 1998). The lake has an important freshwater fishery, although it has been negatively affected by water pollution (Christie, 1974). The food web of the lake has been damaged by over-fishing, changes in the nutrient levels, and various types of pollution, including industrial chemicals, agricultural fertilizers, untreated sewage, and phosphates derived from laundry detergents and other chemicals. These factors have accelerated the eutrophication process by providing nitrogen and phosphorus that promote the rapid growth of competitively dominant plants. Fig. 2 shows Lake Ontario.

Table 1. State variables

Eq	State variable	Description	Initial value	Units
3	c_a	Concentration of phytoplankton	1	mgChla/m^3
13	c_{an}	Concentration of ammonium nitrogen	15	mgN/m^3
17	c_{doc}	Concentration of dissolved organic carbon	0.12	gC/m^3
14	c_{nn}	Concentration of nitrate nitrogen	250	mgN/m^3
16	c_{poc}	Concentration of particulate organic carbon	0.12	gC/m^3
12	c_{srp}	Concentration of soluble reactive phosphorous	12	mgP/m^3
10	c_{zc}	Concentration of carnivorous zooplankton	0.005	gC/m^3
9	c_{zh}	Concentration of herbivorous zooplankton	0.005	gC/m^3

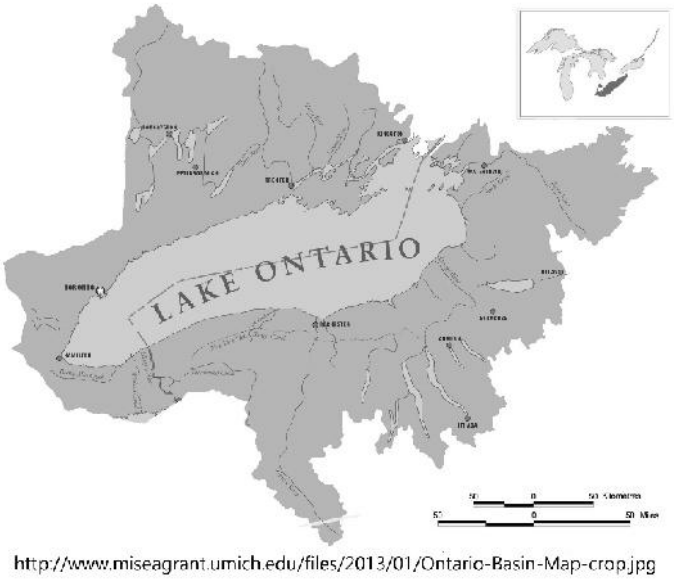

Fig. 2. Lake Ontario

In the model, Lake Ontario was divided into the epilimnion and hypolimnion because of thermal stratification and they were related to each other via diffusion (Fig. 3). Table 2 defines all of the auxiliary variables and their descriptions used in the following equations.

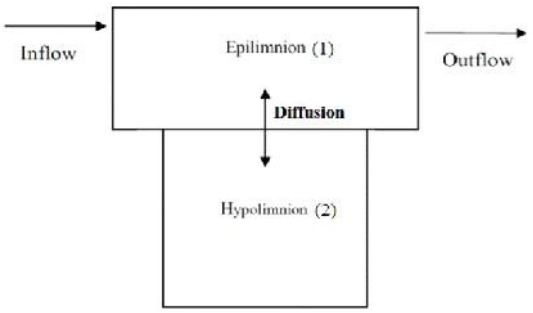

Fig. 3. The physical segmentation scheme and transport representation (Chapra, 1997)

The mass balances for substances present in the epilimnion and hypolimnion can be written as (Chapra, 1997):

$$V_1 \frac{dc_1}{dt} = W(t) - Qc_1 + v_t A_t (c_2 - c_1) + S_1 \quad (1)$$

$$V_2 \frac{dc_2}{dt} = v_t A_t (c_1 - c_2) + S_2 \quad (2)$$

The volumes of the epilimnion and hypolimnion were calculated based on thermal stratification of the Lake. In the model, a state variable was determined to simulate the lake volume with constant epilimnion and hypolimnion volumes. Algae is one of the most important parameters when surveying the qualitative status and eutrophication of lakes (Asmala, 2011; Flynn, 2010). The growth of phytoplankton is a function of the temperature, light, nutrients, algae, and zooplankton. The concentration of algae was represented by the concentration of chlorophyll a. Equation 3 describes the complete model of phytoplankton growth. The concentration of phytoplankton in the hypolimnion was calculated based on deposition from the epilimnion and the diffusivity effect between the two layers (Chapra, 1997).

$$V\frac{dc_a}{dt} = k_{ga}\left(T, c_{tin}, c_{srp}, I\right)Vc_a - k_{ra}Vc_a - r_{gak}(T, c_a, c_{ak})Vc_a + v_a A_t c_{a1} - v_a A_t c_a \quad (3)$$

$$k_{ga}\left(T, c_{tin}, c_{srp}, I\right) = k_{g,20}\,1.066^{T-20}\,¤_L\,¤_N \quad (4)$$

The Michaelis-Menten equation was used to refine the nutrient limitations, as follows:

$$¤_N = \frac{N}{k_{sN} + N} \quad (5)$$

$$¤_N = \min\left\{¤_p, ¤_n\right\} \quad (6)$$

The following equation considers the effect of light limitation on the phytoplankton growth rate.

(7)

$$¤_L = \frac{2.718\,f}{k_e H}\left[\exp\left(-\frac{I_a}{I_s}e^{-k_e H_1}\right) - \exp\left(-\frac{I_a}{I_s}e^{-k_e H_2}\right)\right]$$

$$k_e = k'_e + 0.0088a + 0.054a^{2/3} \quad (8)$$

Fig. 4 shows stock-flow diagram for phytoplankton in eutrophication model.Zooplankton are the main factor affecting the control of phytoplankton growth in the prey-predator cycle (Ramin et al., 2012). Zooplankton are divided into herbivorous and carnivorous zooplankton. The growth of phytoplankton is controlled by herbivorous zooplankton grazing while herbivorous zooplankton growth is limited by carnivorous zooplankton concentration. The zooplankton grazing rate is a function of the temperature, algae, and zooplankton concentration (Chapra 1997; Fasham et al., 1990).

Conspicuously, transporting phosphorous into the cell leads to the maximum growth rate at the maximum organic P quota (P:C) (OPC) as a hyperbolic function of the external phosphate concentration, limited by a hyperbolic function to the maximum size of the inorganic P quota (IPC). Conveying P from IPC to OPC can occur as a hyperbolic function of the accessibility of inorganic P quota (Flynn, 2001). Moreover, it is inhibited when organic P quota reaches its maximum growth capacity. We assume that organic phosphorus is converted into soluble reactive phosphorus, which is used by phytoplankton (Chapra, 1997). Furthermore, as we sought to acquire a simple and reliable model and regarding the reasons asserted in following variable chlorophyll section, s_{pc} is not considered to be one of the main variable ratios. Equation 12 defines the relationships and interactions of soluble reactive phosphorus amongst state variables.

$$V\frac{dc_{zh}}{dt} = \frac{1}{s_{ac}}£_{zh}r_{gzh}(T,c_a,c_{zh})Vc_a - r_{gzc}(T,c_{zc})Vc_{zh} - k_{rzh}Vc_{zh} \quad (9)$$

$$V\frac{dc_{zc}}{dt} = £_{zc}r_{gzc}(T,c_{zc})Vc_{zh} - k_{rzc}Vc_{zc} - k_{dzc}Vc_{zc} \quad (10)$$

$$r_{gzh}(T,c_a,c_{zh}) = \frac{c_a}{k_{sa}+c_a}r_{gzh,20}{}^{T-20}c_{zh} \quad (11)$$

$$V\frac{dc_{srp}}{dt} = s_{pc}k_{ch}Vc_{doc} + s_{pa}k_{ra}Vc_a + s_{pc}k_{rzh}Vc_{zh} + s_{pc}k_{rzc}Vc_{zc} - s_{pc}k_{ga}\left(T,c_{tin},c_{srp},I\right)Vc_a \quad (12)$$

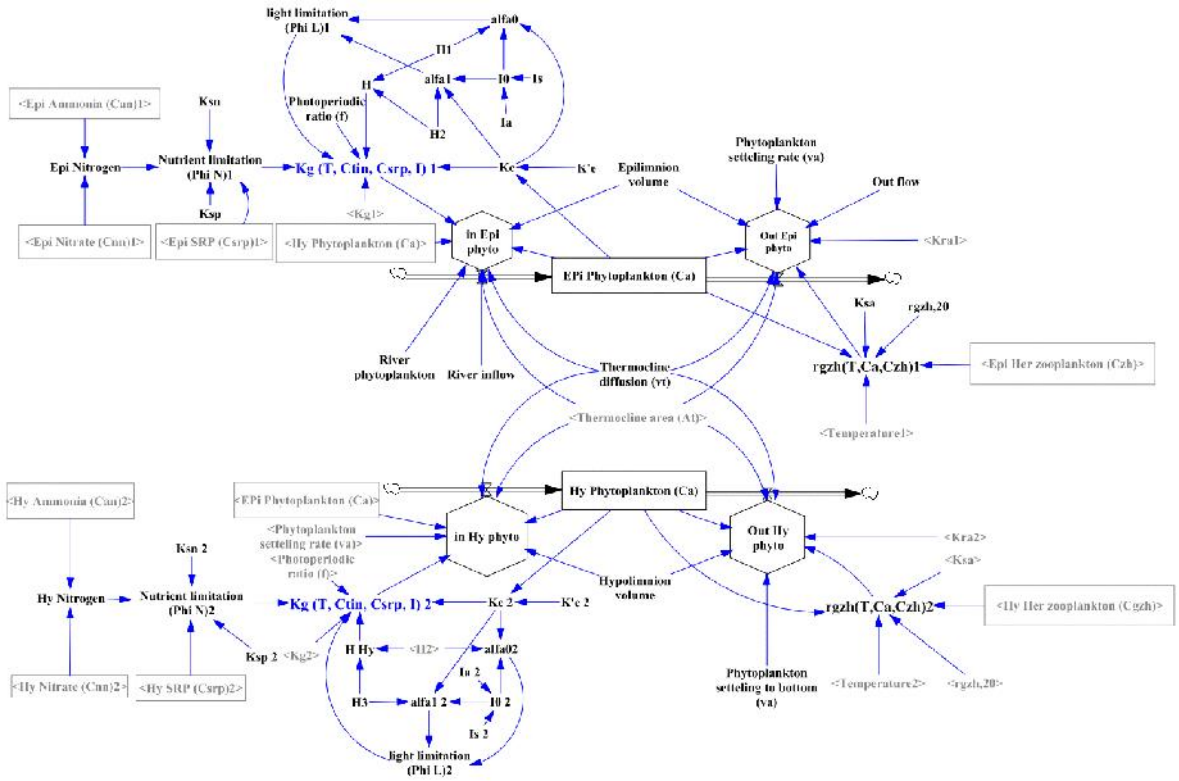

Fig. 4. Stock-flow diagram for phytoplankton

Table 2. Auxiliary variables

Eq	Auxiliary variable	Description	Units
1	c_1	Epilimnion concentration	mg/m^3
1	c_2	Hypolimnion concentration	mg/m^3
3	c_{a1}	Concentration of phytoplankton in epilimnion	mgChla/m^3
18	c_n	Concentration of nitrogen	mg/m^3
3	c_{tin}	Concentration of total inorganic nitrogen= $c_{an} + c_{nn}$	mgN/m^3
13	F_{am}	Fraction of inorganic nitrogen	-
7	H	$= H_2 - H_1$	m
3	I	Daylight Intensity	ly/d[1]
7	I_a	Average light over the daylight hours	-
20	I_{av}	Average irradiance for the layer	ly/d[1]
7	k_e	Extinction coefficient	1/m
3	$k_{ga}\left(T, c_{tin}, c_{srp}, I\right)$	Phytoplankton growth rate	1/d
5	k_{sN}	Nutrient half-saturation constant	-
19	R_C	Respiration rate per cell	gC/cell/d
9	$r_{gzc}\left(T, c_{zc}\right)$	Carnivorous zooplankton grazing rate	1/d
3	$r_{gzh}\left(T, c_a, c_{zh}\right)$	Herbivorous zooplankton grazing rate	1/d
1	S_1	Epilimnion sources and sinks	g/d
2	S_2	Hypolimnion sources and sinks	g/d
9	s_{ac}	The stoichiometric coefficient for the conversion of phytoplankton to carbon	mgChla/gC
13	s_{na}	The stoichiometric coefficient for the conversion of nitrogen to phytoplankton	gN/gChla
13	s_{nc}	The stoichiometric coefficient for the conversion of nitrogen to carbon	gN/gC
12	s_{pa}	The stoichiometric coefficient for the conversion of phosphorous to phytoplankton	gP/gChla
12	s_{pc}	The stoichiometric coefficient for the conversion of phosphorous to carbon	gP/gC
4	T	Temperature	^{o}C
1	t	Time	d
3	V	Volume	m^3
1	$W\left(t\right)$	Loading	g/d
11	¯	Temperature factor	-
18	«	Phytoplankton growth rate	1/d
18	«$_s$	Nutrient - saturated phytoplankton growth rate	1/d
19	«$_{\max}$	Maximum growth rate at saturated light and nutrient level	1/d
4	¤$_L$	Attenuation of growth due to light	-
4	¤$_N$	Attenuation of growth due to nutrient	-
6	¤$_n$	Attenuation of growth due to nitrogen	-
6	¤$_p$	Attenuation of growth due to phosphorous	-

Ammonium and nitrate are vital nutrients for phytoplankton growth (Asmala, 2011; Chapra, 1997). In reality, entering nitrogen into internal nutrient pools due to up taking process is related to the transportation rate of the nitrate and ammonium within the cell. The amino acid glutamine (GLN) consumes the internal ammonium and produces other nitrogenous cellular materials (the nitrogen quota of the cell) (Flynn et al., 1997). The concentration of nitrate is also reduced by converting internal nitrate to ammonium. Nitrogen quota is then utilized to control the cell growth (Flynn & Fasham, 1997). Consequently, feedback and interaction of internal pools are regulated by two crucial factors of maximum pool size and growth rate. To realize the goal of this paper (accomplishing sufficient accuracy based on management purposes) we consider equation 13 and 14 as the prime relations describing feedbacks of nitrate and ammonium with other state variables. In this paper the concentration of internal nitrogen quota is modeled as s_{nc} ratio which is explained in variable chlorophyll section in detail.

The concentration of particulate carbon is affected mainly by carnivorous zooplankton death. Particulate carbon decay increases the concentration of dissolved carbon, which is decreased by hydrolysis (Chapra, 1997).

Most water quality simulation models of water bodies assume constant stoichiometry to facilitate the simulation of the algae and nutrient cycles (Chapra, 1997; Flynn, 2009). However, the growth processes, algae respiration, and nutrient ratio have variable stoichiometry in variable light and nutrient limitation conditions, which has been demonstrated in the qualitative models developed by many researchers (Laws & Chalup, 1990; Goldman, 1986; Li et al., 2012).

Nowadays, the impacts of irradiance and nutrient limitation on light absorption and photosynthetic process besides the relationship between cellular N: C ratios and nutrient-limited growth rates have been in the limelight. In the term of simulating phytoplankton growth, there are three basic approaches of Monod, Quota and Mechanistic (Flynn, 2003a). The Monod model explains that the growth rate is a direct function of the external nutrient concentration as a rectangular hyperbolic (RH) function besides light is either non-limiting or its level of limitation is invariant (Monod, 1949). Thus, once one nutrient is exhausted, the growth of phytoplankton ceases instantly. Although the Quota approach is also a function of the external nutrient, it considers the internal nutrient content (the quota) as the limiting factor (Droop, 1968, 1973; Caperon & Meyer, 1972). This model can be more realistic sine it is capable of considering the continuing growth in the absence of external nutrients. In the certain approach, uptake regulates the growth on account of the maximum demand of cell under non-limiting nutrient concentration which is unrealistic to argue because uptake is controlled by feedback from cellular biochemical processes (Flynn, 2003a). The Mechanistic model deals with feedbacks and interactions of nutrients associated with algal growth. Additionally, in this method, it is attempting to develop a comprehensive structure to take every process into account on biochemical knowledge. The more complicated mechanistic model is utilized, with feedback processes and perhaps multiple internal pools, the more strictly biochemical reality can be attained in outputs (Flynn, 2003b). In contrast, it should be noted that not only can boosting complexity in such model avoid enhancing reliability, but also it can strengthen the uncertainty and cost of the model

$$V\frac{dc_{an}}{dt}=s_{nc}k_{ch}Vc_{doc}+s_{na}k_{ra}Vc_{a}+s_{nc}k_{rzh}Vc_{zh}+s_{nc}k_{rzc}Vc_{zh}-F_{am}s_{nc}k_{ga}\left(T,c_{tin},c_{srp},I\right)Vc_{a}-k_{n}Vc_{an} \tag{13}$$

$$V\frac{dc_{nn}}{dt}=k_{n}Vc_{an}-\left(1-F_{am}\right)s_{na}k_{ga}\left(T,c_{tin},c_{srp},I\right)Vc_{a} \tag{14}$$

$$F_{am}=\frac{c_{an}}{k_{am}+c_{an}} \tag{15}$$

$$V\frac{dc_{poc}}{dt}=\frac{1}{s_{ac}}\left(1-£_{zh}\right)r_{gzh}(T,c_{a},c_{zh})Vc_{a}-\left(1-£_{zc}\right)r_{gzc}(T,c_{zc})Vc_{zh}+k_{dzc}Vc_{zc}$$
$$-k_{cp}Vc_{poc}+v_{cp}A_{t}c_{poc1}-v_{cp}A_{t}c_{poc}\frac{n!}{r!\left(n-r\right)!} \tag{16}$$

$$V\frac{dc_{doc}}{dt}=k_{cp}Vc_{poc}-k_{ch}Vc_{doc} \tag{17}$$

(Chapra, 1997). What is more to the approaches described, other structures which are not too readily categorized as three famous approaches exist. Laws and Chalup (1990) developed N-light interaction model based on Shuter's (1979) model demonstrating the partitioning of cellular C amongst metabolic and storage pools. Lancelot et al. (2000) also made use of Shuter's method to explain N-Si-Fe-light interactions. However, their model consists of a Mechanistic approach to characterize the partitioning of intracellular C, feedback processes with nutrients conformed to a Monod structure (Lancelot et al., 2000). Solving simultaneous equations is applied to calculate Chl a:C by balancing light and nutrient limitations at each time step (Flynn, 2001).

According to the above explanation, a paramount hurdle to the development and testing of models is the absence of compatible data and a suitable time to increase simultaneously the complexity and reliability of the simulation model under varied multi-factorial circumstances. Thus, the chief goal set in this paper is to model algal growth process with adequate reliability compared to consider constant stoichiometry approach in order to integrate into water quality frameworks with quite complexity. Laws and Chalup (1990) have indicated that under N-limited conditions, the N:C ratio is exclusively associated with the relative growth of cells. A cell encountering lack of an external source of P will redistribute P since phosphorus can be accumulated to adequate levels into cells and appropriate growth rates may last for a couple of generations. However, phytoplankton is incapable of accumulating sufficient internal inorganic N to guarantee growth rates (Joseph & Villareal, 1998). Furthermore, making use of such factors depends on the structure and application of the model, and the time horizon of the scenarios. Therefore, in this paper, we considered a linear relationship between N: C and relative growth rate (μ/μs), a hyperbolic relationship between nutrient-saturated growth rates and irradiance, and a linear relationship between growth rate and both respiration rate and Chl a:C ratios according to Laws and Chalup (1990) equations. Laws and Chalup 1990 defined the variable chlorophyll model as follows (Laws & Chalup, 1990):

Fig. 5 shows a diagram of the computational model of the variable stoichiometry coefficients. The values and definitions of all the constants used in the eutrophication model are summarized in Table 3. To analyze the model behavior and measure the amount and impact of the parameters on the model's output, the sensitivity analysis of the model was conducted. In this regard, in each modeling, the effect of each parameter's fluctuations was measured, while other parameters were kept constant. Therefore, the relative sensitivity factor was calculated for recognizing the most effective parameters on the model (Shirmohammadi et al., 2006).

Which in it, "O" is the model's output, and "P" is the studied input parameter. The model's parameters were calibrated manually by making use of the trial and error method based on the available amounts in a wide variety of worthwhile probs. Table 4 indicates the model's sensitivity analysis for an average concentration of phytoplankton. The sensitivity coefficient outcomes revealed that the factors mostly effecting the lake's phytoplankton concentration were the algae growth rate, phytoplankton decay rate, light extinctioný, and the herbivorous zooplankton grazing rate. The range of parameters alters on account of the trials and errors, and the closeness of the model's average output and the observed data.

$$\ll_s = \frac{K_e(1-r_g)(1-S/C)I}{K_e/f_{p0} + I\left[1+K_e/\left(k_{si}f_{p0}\right)\right]} - r_0/C \qquad (18)$$

$$R_C = \left(r_0/C + r_g\ll\right) = 0.042 + 0.389\ll_{\max}\frac{\ll}{\ll_s}\frac{I}{k_{si}+I} \qquad (19)$$

$$s_{nc} = \left[F + (1-F)\ll/\ll_s\right]/W_N = 32 + 113\frac{\ll}{\ll_s} \qquad (20)$$

$$s_{ac} = \left\{1-(1-F)(1-\ll/\ll_s) - S/C - (\ll + r_0/C)/\left[(1-r_g)K_e\right]\right\}\Big/ W_{Chl} = 6.4 + 45\frac{\ll}{\ll_s}\frac{k_{si}}{k_{si}+I_{av}} \qquad (21)$$

$$F_{sa} = \frac{\partial O}{\partial P}\times\frac{P}{O} \qquad (22)$$

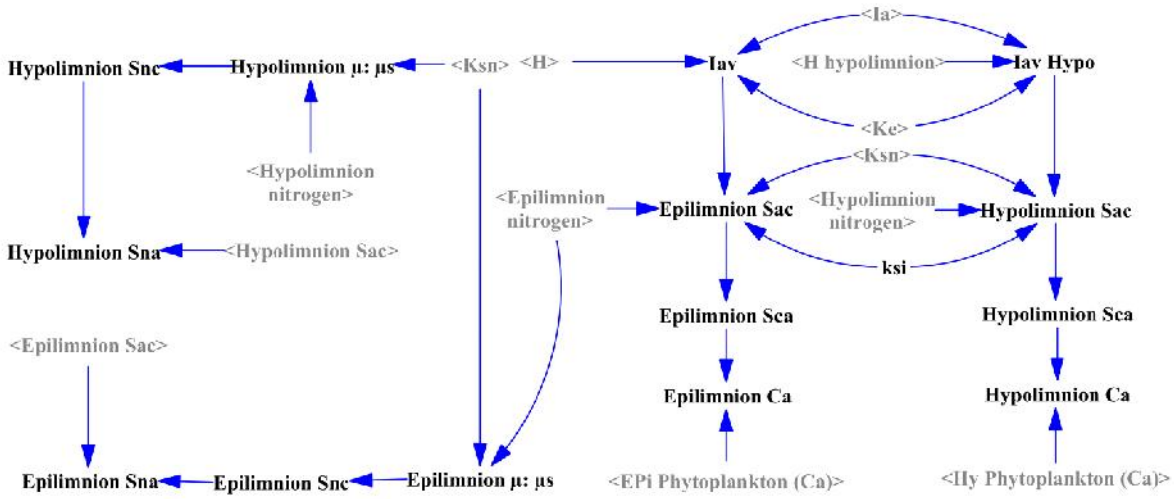

Fig. 5. Diagram showing the computational model of the variable stoichiometry coefficients

After analyzing the sensitivity, the developed phosphorous cycle was applied on the data acquired from the Ontario lake, and the model's error was measured using the Nash-Sutcliff efficiency coefficient, the Pierson correlation coefficient, and the standard error. Nash-Sutcliff efficiency is defined as equation 23:

$$E_{ns} = 1 - \left(\sum (C_o - C_m)^2 \Big/ \sum (C_o - C_{oave})^2 \right) \quad (23)$$

Where C_o is observed variable and C_m is simulated variable. Nash–Sutcliffe efficiencies can range from $-\infty$ to 1. An efficiency of 1 (E = 1) corresponds to a perfect match of estimated outcomes to the observed data. An efficiency of 0 (E = 0) indicates that the model predictions are as precise as the mean of the observed data, whereas an efficiency less than zero (E < 0) occurs when the observed mean is a better predictor compared with the model or, in other words, when the residual variance, is larger in comparison to the data variance (Nash & Sutcliff, 1970). According to Table 5, the appropriate accordance of the model's output with the observed data is indicated by a close to 1 Nash-Sutcliff coefficient (E_{ns}), the data correlation coefficient (R^2), and also the low standard errors for the model's calibration and verification periods. This matter denotes a reliable model definition. Fig. 6 shows observed data and simulation results for phytoplankton in epilimnion and hypolimnion of Lake Ontario. It can be seen that the correlation between estimated and observed data for phosphorus is very close in both layers.

Specific tests can distinguish the weak points of the built models, based on the system dynamics logic presented by the model builders; a couple of which are pointed out below. Conspicuously, the units of each state variable, and the covariates related to the entire model were analyzed using the Units Check order, and should there are any inconsistencies in units throughout the model, we will encounter an error. In addition it must be argued that should there is a dimensional consistency error, outcomes will not suffer from flaw during the modeling. Nevertheless, it is easier to track the varied predicaments so as to tackle feasible hardships during the modeling. In this study, the simulation model did not suffer from dimensional inconsistencies errors. With the expansion of the model, the extreme circumstances during simulation period should be tackled. For this reason, the input load and initial concentration of soluble reactive phosphorous, ammonium and nitrate as well as phytoplankton load were considered at 0. Accordingly, fig. 7 reveals that the phytoplankton concentration moves towards 0.4, from the initial amount of 1 (mg Chla per cubic meters).

RESULTS & DISCUSSION

To assess the effect of variable stoichiometry on the eutrophication model, Lake Ontario was simulated using daily time steps for one year. The initial levels of the state variables were considered to be their concentrations at the start of the simulation. This section presents the results of the main eutrophication model parameters including phytoplankton, herbivorous and carnivorous zooplankton, ammonium, nitrate, particulate and dissolved carbon, and soluble reactive phosphorus for the epilimnion with constant and variable stoichiometry.

The overall behaviors of the state variables were studied throughout the year using a seasonal modeling approach (i.e., temperature, day length, light intensity,

Table 3. Constants

Constan	Definition	Value	Unit	Constant	Definition	Value	Unit
A_s	Surface area	$19*10^9$	m^2	A_t	Thermocline area	$10*10^9$	m^2
H_1	Epilimnion thickness	20	m	H_2	Hypolimnion thickness	82	m
I_s	Optimal light level	350	ly/d	k_{ch}	Nonliving carbon hydrolysis rate	0.075	1/d
k_n	Nitrification rate	0.1	1/d	Q	Outflow	$212*10_9$	m^3/yr
V_1	Epilimnion volume	$254*10^9$	m^3	V_2	Hypolimnion volume	$138*10_{10}$	m^3
r_0/C	Basal respiration rate	0.03	1/d	f	Photoperiod	Time Series	-
v_a	Phytoplankton settling velocity	0.2	m/d	v_{cp}	Nonliving carbon settling velocity	0.2	m/d
k_{cp}	Dissolution rate for nonliving carbon	0.1	1/d	k_{dzc}	Carnivorous zooplankton death rate	0.04	1/d
k_{sa}	Phytoplankton half-saturation constant	10	µgChl a/L	k_{si}	Light half-saturation constant	64	mol quanta/m^2/
k_{sp}	Phosphorous half-saturation constant	2	µgP/L	k_{sn}	Nitrogen half-saturation constant	15	µgN/L
t_{es}	End of stratification	20	d	t_{oes}	Onset of end of stratification	315	d
t_{tes}	Time of establishing stratification	58	d	t_{sss}	Start of summer stratification	100	d
$£_{zc}$	Carnivorous zooplankton grazing efficiency	0.7	-	$£_{zh}$	Herbivorous zooplankton grazing	0.7	-
$r_{gzc,20}$	Carnivorous zooplankton grazing rate @ T=20 °C	5	L/mg C/d	S/C	Structural carbon per total carbon	0.1	-
k_{ra}	Phytoplankton losses due to respiration and	0.025	1/d	k_{rzc}	Carnivorous zooplankton losses due	0.04	1/d
k_{rzh}	Herbivorous zooplankton losses due to respiration	0.1	1/d	$r_{gzh,20}$	Herbivorous zooplankton grazing	5	L/mgC/d
$k_{ga,20}$	Phytoplankton growth rate @ T=20 °C	2	1/d	k_{am}	Half-saturation constant for ammonium	50	µgN/L
K_e	Gross photosynthesis rate per unit quantity of dark reaction carbon	3.6	1/d	k'_e	Light extinction due to factors other than phytoplankton	0.2	1/m
r_g	Rate of change of respiration rate per unit change in gross	0.28	gC/cell/d	W_{Chl}	Ratio of total cell C/Chl a in the light reaction component of Carbon	17	gC/gChla
F	Quotient of nutrient limited N/C ratios at relative gross rate of 0 and 1	0.22	-	W_N	Ratio of total cell C/N in structure, light/dark reaction of Carbon	6.9	gC/gN
f_{p0}	Value of gross rate of photosynthesis per unit light reaction carbon per unit light intensity in the limit of zero irradiance	0.28	m^2mol/quanta	v_t	Thermocline diffusion: Summer-stratified Winter-stratified	0.13 13	cm^2/s

etc.) because there were similar changes in the behaviors of the parameters using both simulation approaches. The causes of differences in the variable concentrations were studied using constant and variable stoichiometry approaches. Figure 8 shows the temperature and light data for Lake Ontario. According to Fig. 9, the phytoplankton growth rate increased slightly during the first two months of the year because of the gradual reduction in the temperature, a gradual increase in the light, and the photoperiodic ratio (Fig. 8). These factors approximately neutralized and controlled the growth of phytoplankton. The phytoplankton activity levels increased abruptly due to the lack of nutrient limitations when there was a dramatic rise in the temperature and solar radiation, and the phytoplankton concentration reached a peak on about Day 160 when the summer stratification developed (Fig. 9).

Table 4. The sensitivity coefficient of the phytoplankton concentration in the lake

Parameters	**Symbol**	**Variation range**	F_{sa}
Phytoplankton growth rate	$k_{ga,20}$	0.8 – 2.1	0.623
Phytoplankton losses due to respiration and excretion	k_{ra}	0.02 – 0.04	-0.572
Light extinction due to factors other than phytoplankton	k_e'	0.1 - .0.4	0.532
Herbivorous zooplankton grazing rate	$r_{gzh,20}$	4 – 6	0.323
Parameters	Symbol	Variation range	F_{sa}
Phytoplankton growth rate	$k_{ga,20}$	0.8 – 2.1	0.623
Phytoplankton losses due to respiration and excretion	k_{ra}	0.02 – 0.04	-0.572
Light extinction due to factors other than phytoplankton	k_e'	0.1 - .0.4	0.532
Herbivorous zooplankton grazing rate	$r_{gzh,20}$	4 – 6	0.323

Table 5. The results of Nash-Sutcliff coefficient, correlation coefficient, and the standard error

Criterion	**R^2**	**S_e**	**E_{ns}**
Epilimnion phytoplankton	0.9888	0.9674	0.9805

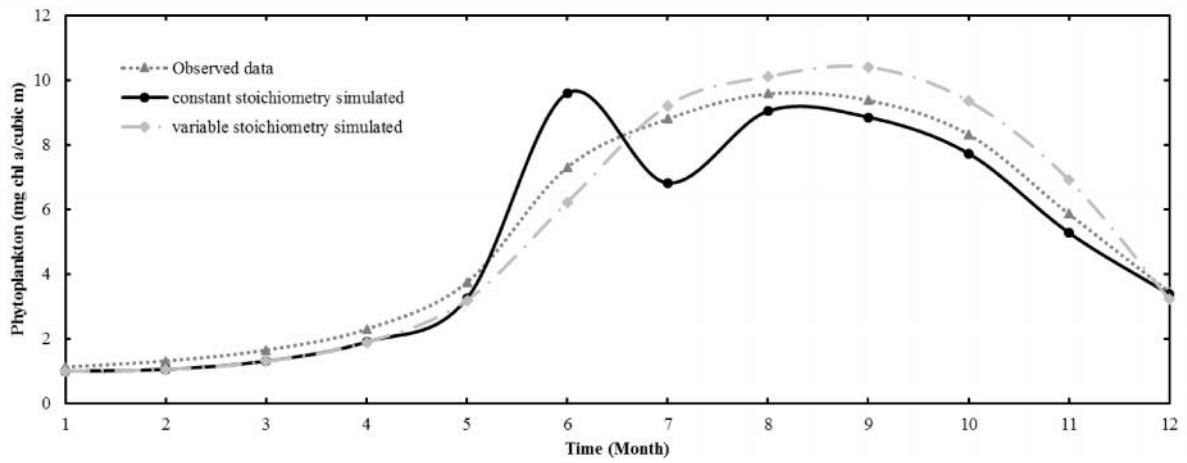

Fig. 6. The observed and simulated concentrations of the phytoplankton

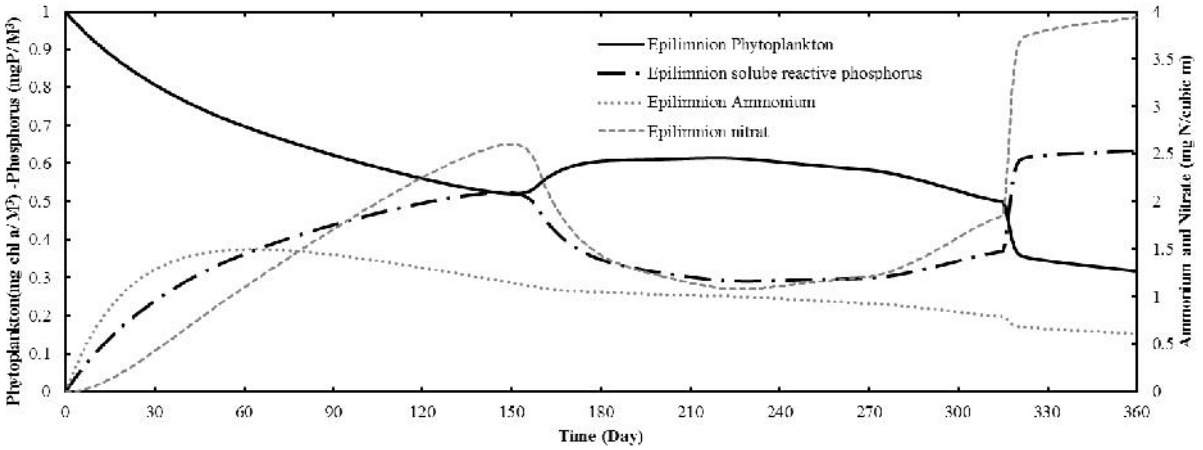

Fig. 7. The results of state variable concentration under extreme conditions

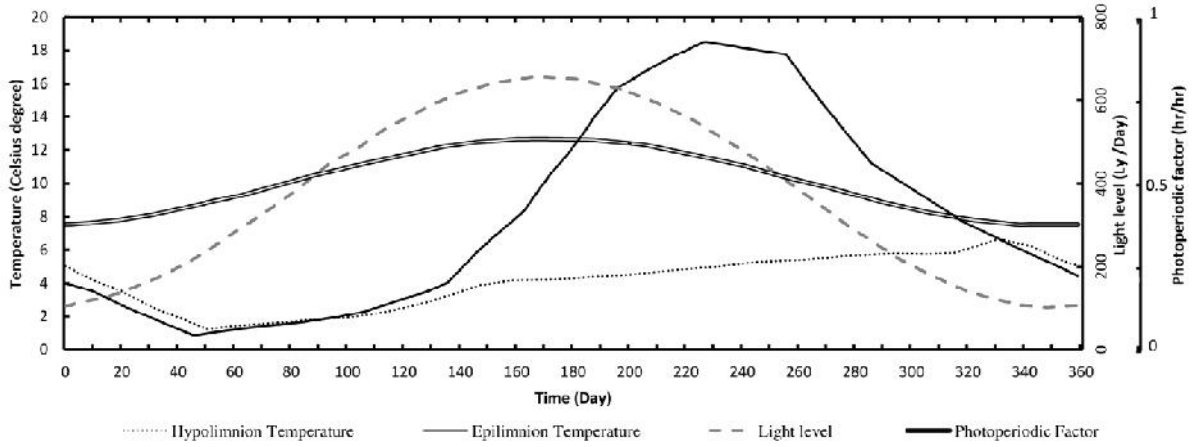

Fig. 8. Temperature and light data for Lake Ontario (Chapra, 1997)

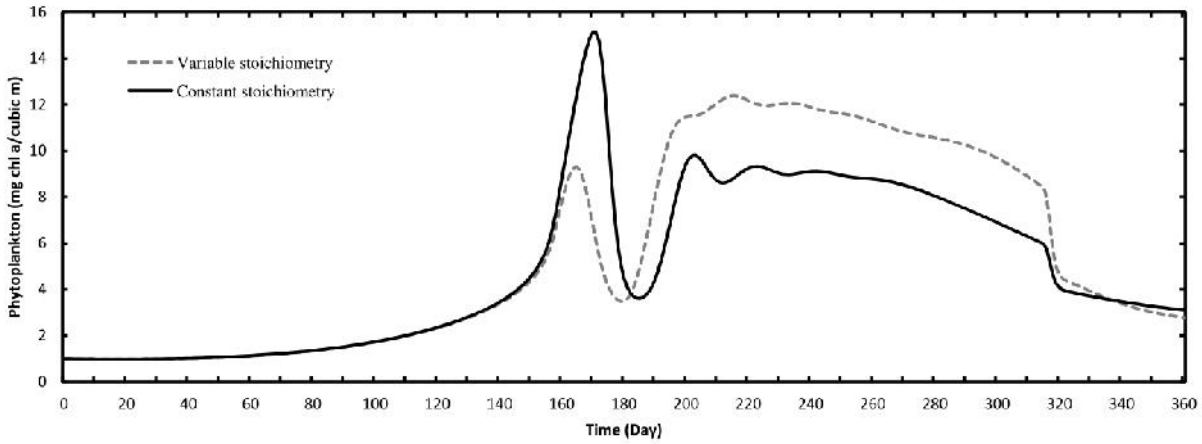

Fig. 9. Phytoplankton concentration using constant and variable stoichiometry simulation

Figs 10 and 11 showed that the nutrient concentrations increased slowly because of the slow growth of algae, the continued entry of nutrients, and the decline in the temperature. Thus their concentrations declined rapidly as the algal growth increased. Minimum of ammonium concentration occurred at about Day 180 when the phytoplankton concentration peaked. Afterward, its concentration increased as a consequence of the phytoplankton growth limitation and the respiration of phytoplankton, zooplanktons, and carbons. Eventually, declining in such concentrations may lead to gradually reduction of ammonium concentration.

However, the variations of nitrate and phosphorus concentration were similar to the variations of ammonium concentration; they were increased during last months of the year because of the decreased in the stratification condition and nitrification for nitrate concentration. The concentration of zooplankton increased with their grazing and the concentration of herbivorous zooplankton peaked on about Day 180 due to the time delay in the prey-predator cycle (Fig. 12). The maximum level of zooplankton grazing occurred at this time and the concentration of phytoplankton declined dramatically as a consequence. Therefore, the oscillations generated in the system may be attributed to the control of algal growth by herbivorous zooplankton.

Similar to the herbivorous zooplankton growth process, the carnivorous zooplankton concentration reached a maximum on about Day 190, before decreasing gradually (Fig. 12). Decreased in light intensity and temperature had direct effect on the declination of phytoplankton activity levels. Therefore, the nutrient concentrations softly increased in the epilimnion. The concentrations of particulate and dissolved carbon were similar to the zooplankton concentrations since they were the source of carbons. Thus, carbons storages gradually declined because of low zooplankton grazing during the first five months of the year. The concentrations of particulate carbon reached a maximum at about Day 190 and the concentration of dissolved carbon increased as a consequence (Fig. 13).

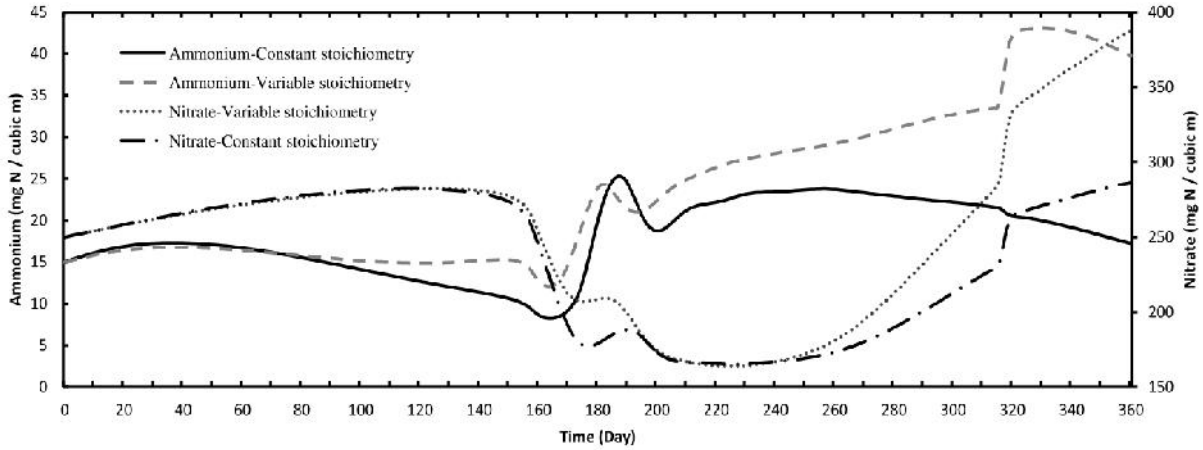

Fig. 10. Ammonium and nitrate concentration using constant anvariable stoichiometry simulation

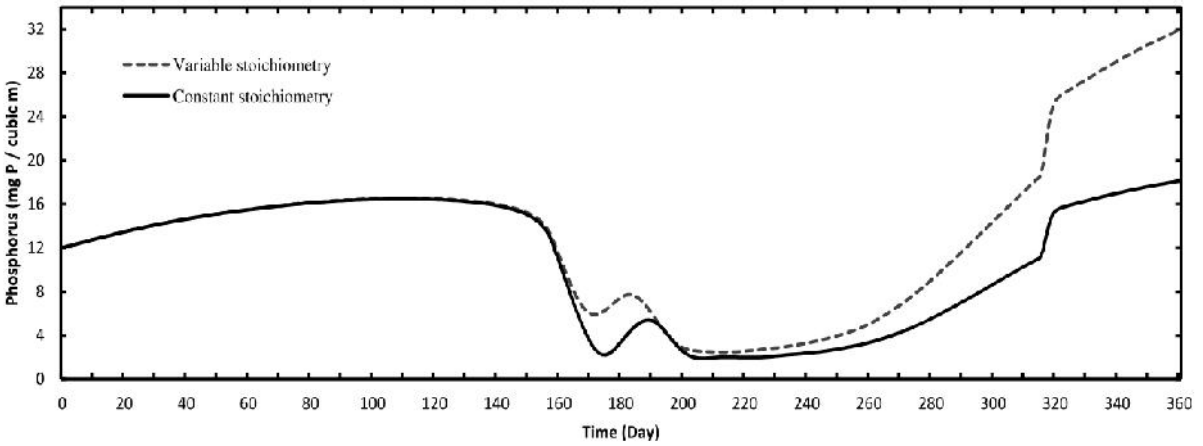

Fig. 11. Soluble phosphorus concentration using constant and variable stoichiometry simulation

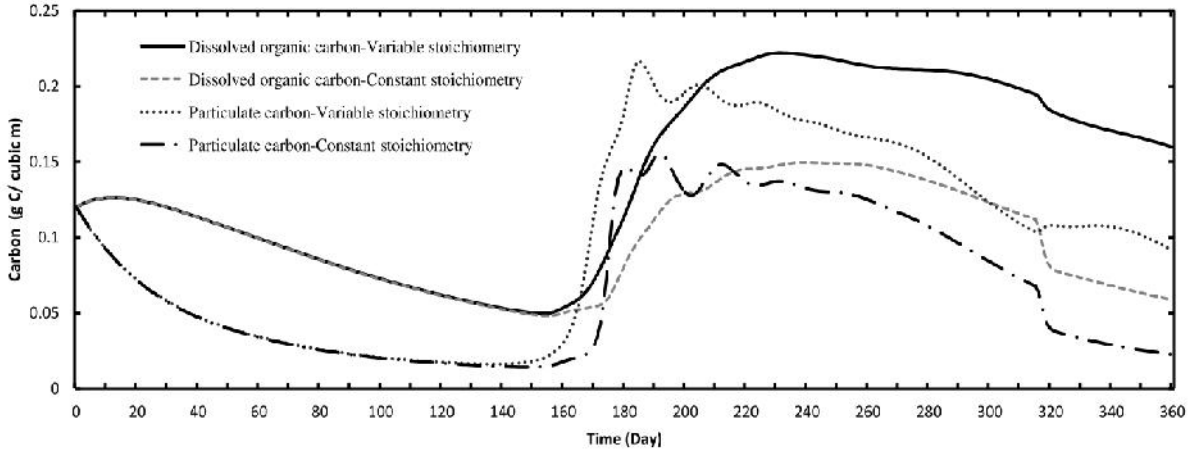

Fig. 12. Herbivorous and carnivorous zooplankton concentration using constant and variable stoichiometry simulation

Strong vertical mixing occurred during the late summer when the phytoplankton concentration declined and the nutrient concentrations increased. This situation led to the fluctuations of the carnivorous zooplankton concentration in the final days of the year.

The differences and changes in the parameter concentrations must be known to describe the behavior of state variables in constant and variable stoichiometry simulations of the epilimnion. Identifying these parameters presents certain difficulties from the

perspective of tracing the effects of variable feedback relationships because of the model complexity and the many causal relationships. According to the prey-predator cycle equation, the carbon to chlorophyll a ratio (S_{ac}) has a critical role in the conversion of algae to zooplankton, dissolved carbon, and particulate carbon. Thus, the fluctuations in this ratio need to be studied initially, before the nitrogen to carbon (S_{nc}) and nitrogen to chlorophyll a (S_{na}) ratio are investigated, which have direct effects on the ammonium and nitrate concentrations.

Based on Equation 9, S_{ca} has a direct relationship with the herbivorous zooplankton concentration, so changing the S_{ca} affected the carnivorous zooplankton concentration indirectly. The phytoplankton concentration was also affected by these changes and the process continued until it reached equilibrium (Fig. 9).

Fig. 14 shows the trend in S_{ac} using constant and variable simulation approaches. The relationship between nutrient and light is described in the equation 21. This ratio decreased with nutrient concentrations whereas it increased when there was an increase in the light intensity. Fig. 15 shows the trends in light and nutrients as limiting factors. The trend of the S_{ac} changes was similar to that of the light changes. The decrease and then increase in this ratio were functions of light enhancement from the start of the year to midsummer, followed by its decline. The oscillation in the ratio about Day 180 was also caused by fluctuations in the light extinction coefficient due to variations in the concentration of algae (Equation 8).

Thus, the reduction in the peak algae concentration and the minimization of its concentration on about Day 180 in the variable stoichiometry simulation was due to the increased herbivorous zooplankton and its controlling role. It should be noted that the effect of nutrient limitation was considered in the S_{ac} diagram, but the value of nutrient limitation was close to one so the S_{ac} behavior followed the light limitation trend. According to Fig. 16, the S_{nc} changes were about 137–141 mg N/g C, which was about 20% less than the amount (180 mg N/g C) in the constant stoichiometry approach (Chapra 1997). Therefore, the ammonium concentration decreased by about 20% when its effect was measured while keeping the remaining parameters constant. The validity of this was evaluated further and confirmed. Given the variability of S_{ac} in the main model, however, the ammonium behavior had changed and there was no reduction in its concentration. The S_{na} ratio was obtained by dividing S_{nc} by S_{ac} (Fig. 14).

The simulation period was divided into two sections to facilitate interpretation of the results. The first section started at the beginning of the year and continued until the first sharp drop (about Day 160) while the second started after this point and continued until the end of the year. There were two key points in the assessment of the phytoplankton concentration as follows: a) S_{ac} decreased steeply from the start of the simulation until about Day 180 (with the fluctuations of approximately 20–38 (mg Chla/ g C) over the year) (Fig. 14). Thus, the herbivorous zooplankton concentration was slightly more than that when the stoichiometry was constant (Fig. 13); b) the herbivorous zooplankton concentration increased slowly from the start until it increased dramatically at Day 170 for the constant stoichiometry simulation mode (Fig. 13). S_{ac} was lower than that with the constant stoichiometry approach (3Fig. 13), so the peak in the herbivorous zooplankton concentration (0.31 g C/m^3) was more than that in the constant stoichiometry simulation (0.29 g C/m^3). Thus, the reduction in the peak phytoplankton concentration and the minimization of its concentration on about Day 180 in the variable stoichiometry simulation was due to the increased herbivorous zooplankton and its controlling role.

The analysis of the trend in the carnivorous zooplankton concentration during the first period showed that, because of the change in the time of the increase in the herbivorous zooplankton concentration, the rise in the carnivorous zooplankton concentration occurred earlier (about Day 160) due to zooplankton grazing (Fig. 16). The carnivorous zooplankton reached a peak at Day 180 and simultaneously there was a huge drop in the herbivorous zooplankton concentration. There was also an increase in the algae concentration between Day 180 and Day 210 in the simulation. The higher algae concentration during the second period of the variable stoichiometry simulation compared with the constant approach may have two explanations, i.e., the increase in S_{ac} and the controlling role of carnivorous zooplankton during this time period (Fig. 9). In addition, the higher concentration of carnivorous zooplankton in the variable stoichiometry simulation may have been due to the higher concentration of herbivorous zooplankton during the initial period. The light and temperature declined from around Day 210 and the prey-predator concentrations also decreased. Finally, the completely mixed condition was established at around Day 320 (Fig. 9).

The fluctuations in the ammonium concentration during the first period were lower and its concentration was higher than that with the constant stoichiometry because of the algae concentration reduction, whereas the S_{nc} and S_{na} ratios increased (Fig. 10). The greater increase in the ammonium concentration compared with the constant stoichiometry may due to the thermal

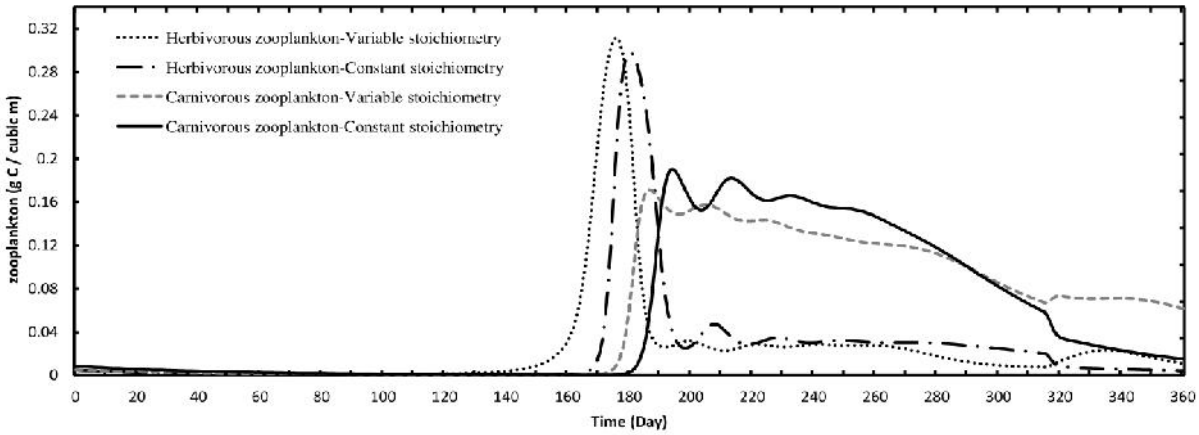

Fig. 13. Dissolved and particulate organic carbon concentration using constant and variable stoichiometry simulation

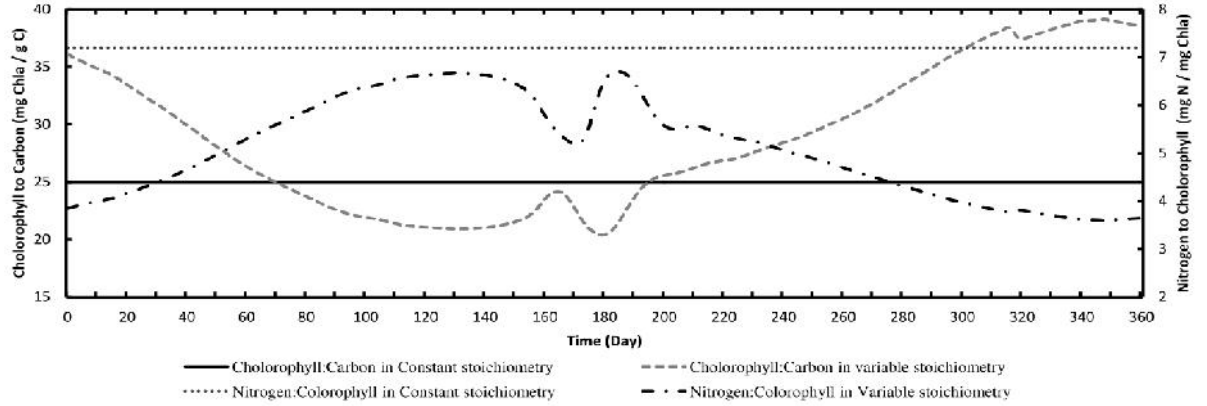

Fig. 14. Chlorophyll-a to carbon and nitrogen to colorophyll ratio

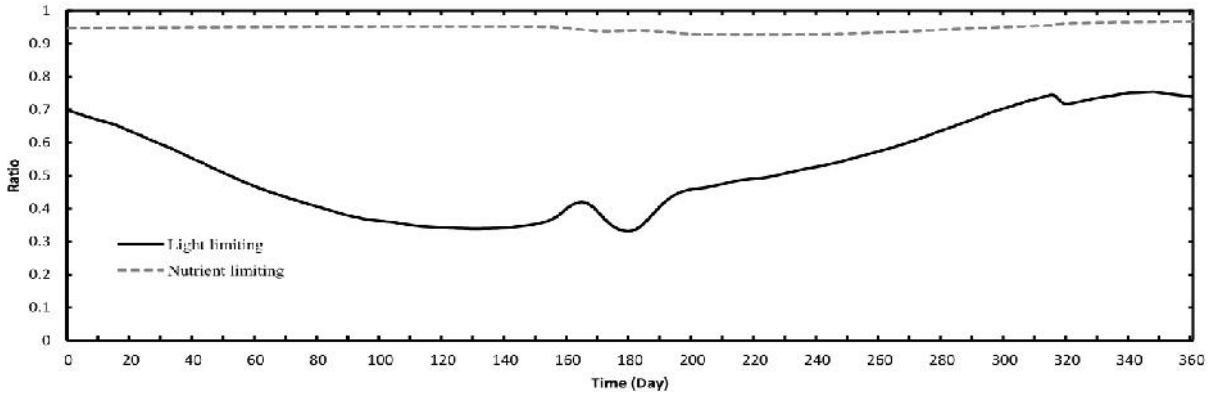

Fig. 15. Light and nutrients as limiting factors

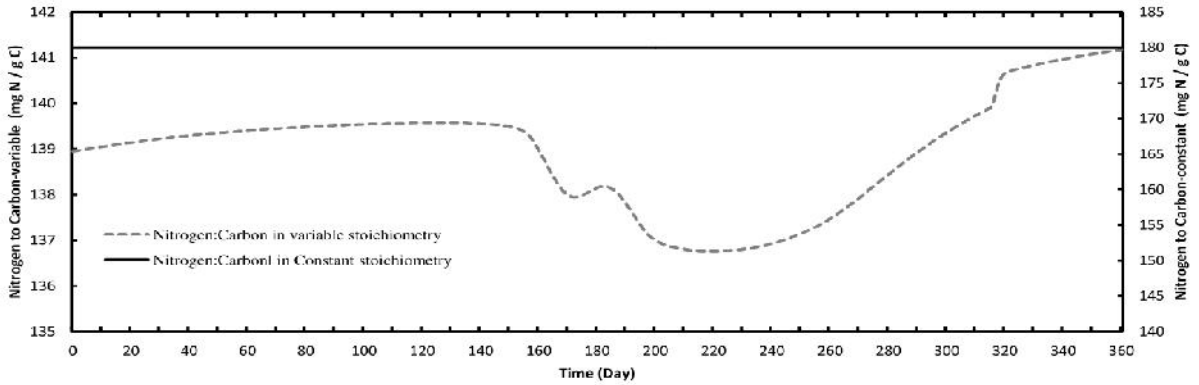

Fig. 16. The nitrogen to carbon ratio

stratification, the phytoplankton growth decline, and the zooplankton decay. The S_{nc} decline during the second period was considered in the model, but it had no significant effect in the ammonium behavior diagram (Fig. 10) because of the significant increase in the zooplankton concentration (Equation 13). The behavioral differences in the phosphorus and nitrate concentrations reduced phytoplankton growth due to declines in the temperature, light, photoperiodic ratio, and zooplankton grazing (Figs. 9, 10). The particulate and dissolved carbon concentration variations were highly vulnerable to fluctuations in the zooplankton concentration, which was the main cause of the differences between the two simulation approaches.

CONCLUSIONS

In this study, a eutrophication model of a lake was simulated utilizing constant and variable stoichiometry with a system dynamics approach. The simulation time interval was divided into two sections to facilitate explanations of the behaviors of variables affected during eutrophication. The overall trends and fluctuations in the variable concentrations were assessed in the first section and the second section. The influences of variable stoichiometry on the state variable concentrations and the causes of the difference with constant stoichiometry were evaluated. Despite the similar overall behavior of the system in the two simulation approaches, the results revealed that the extreme levels of the algal bloom were varied and they were lower in the variable stoichiometry simulation. It is of paramount significance to note that changes in the algal growth rate boosted the probability of the extreme conditions occurring over time. This could have a direct impact on decision making by water quality managers to control eutrophication outcomes. Another output of this study was the development of a training-based model for simulating eutrophication, which have ability to evaluate and analyze this highly complex environmental phenomenon with an appropriate level of precision, while providing the flexibility to investigate various changes in the model circumstances. The application of such model to water quality management would provide an interactive learning environment for modelers, decision-makers, and operators who intend to enhance the effectiveness of quality management policies.

REFERENCES

Afshar, A., Saadatpour, M. and Marino, M.A. (2012). Development of a complex system dynamic eutrophication model: application to Karkheh reservoir. Environmental Engineering Science, **29(6),** 373-385.

Agency, U.S.E.P. (1998). Great Minds?, Great Lakes!, Lake Guardian, Don't Miss The Boat With Environmental Education.

Ahmad, S. and Simonovic, S.P. (2004). Spatial system dynamics: new approach for simulation of water resources systems. Journal of Computing in Civil Engineering, 18(4), 331–340.

Ahmad, S. and Simonovic, S.P. (2006). An intelligent decision support system for management of floods. Water Resources Management, **20(3),** 391–410.

Andersen, J.H., Schlüter, L. and Ærtebjerg, G. (2006). Coastal eutrophication: recent developments in definitions and implications for monitoring strategies. Journal of Plankton Research, **28(7),** 621–628.

Anderson, D.M., Glibert, P.M. and Burkholder, J.M. (2002). Harmful algal blooms and eutrophication: nutrient sources, composition, and consequences. Estuaries, **25,** 704–726.

Asmala, E., Saikku, L. and Vienonen, S. (2011). Import–export balance of nitrogen and phosphorus in food, fodder and fertilizers in the Baltic Sea drainage area. Science of the Total Environment, **409(23),** 4917-4922.

Bowie, G.L., Mills, W.B., Porcella, D.B., Campbell, C.L., Pagenkopf, J.R., Rupp, G.L., Johnson, K.M., Chan, PWH, Gherini, S.A. and Chamberlin, C.E. (1985). Rates, constants, and kinetics formulations in surface water quality modeling. EPA, **600,** 3-85.

Caperon, J. and Meyer, J. (1972). Nitrogen-limited growth of marine phytoplankton. I. Changes in population characteristics with steady-state growth. Deep Sea Research, **19,** 601-18.

Chapra, S.D. (1997). Surface water quality modeling. 1th Edition, Mc Graw-Hill, Inc.

Christie, W.J. (1974). Changes in the fish species composition of the Great Lakes. Journal of the Fisheries Research Board of Canada, **31,** 827–54.

Davidson, K., Gowen, R.J., Tett, P., Bresnan, E., Harrison, P.J., McKinney, A., Milligan, S., Mills, D.K., Silke, J. and Crooks, A.M. (2012). Harmful algal blooms: how strong is the evidence that nutrient ratios and forms influence their occurrence? Estuarine, Coastal and Shelf Science.

Droop, M.R. (1968). Vitamin B 12 and marine ecology. IV. The kinetics of uptake, growth, and inhibition in Monochrysis lutheri. Journal of the Marine Biological Association of the United Kingdom, **48,** 689-733.

Droop, M.R. (1973). Some thoughts on nutrient limitation in algae. Journal of Phycology, **9,** 264-72.

Elshorbagy, A. and Ormsbee, L. (2006). Object-oriented modeling approach to surface water quality management. Environmental Modeling Software, **21(5),** 689–698.

Fasham, M., Ducklow, H. and McKelvie, S.M. (1990). A nitrogen-based model of plankton dynamics in the oceanic mixed layer. Journal of Marine Research, **48(3),** 591-639.

Flynn, K.J. and Fasham, M.J.R. (1997). A short version of the ammonium-nitrate interaction model. Journal of Plankton Research, **19,** 1881-1897.

Flynn, K.J. (2001). A mechanistic model for describing dynamic multi-nutrient, light, temperature interactions in phytoplankton. Journal of Plankton Research, **23,** 977–997.

Flynn, K.J. (2003a). Modelling multi-nutrient interactions in phytoplankton; balancing simplicity and realism. Journal of Progress in Oceanography, **56,** 249– 279.

Flynn, K.J. (2003b). Do we need complex mechanistic photoacclimation models for phytoplankton? Journal of Limnology and Oceanography, **48,** 2243-2249.

Flynn, K.J. (2005a). Modelling marine phytoplankton growth under eutrophic conditions. Journal of Sea Research, **54(1),** 92-103.

Flynn, K.J. (2005b). Castles built on sand: dysfunctional plankton models and the failure of the biology-modeling interface. Journal of Plankton Research, **27,** 1205–1210.

Flynn, K.J. (2010). Ecological modelling in a sea of variable stoichiometry; dysfunctionality and the legacy of Redfield and Monod. Progress in Oceanography, **84,** 52–65.

Flynn, K.J., Clark, D.R. and Xue, Y. (2008). Modelling the release of dissolved organic matter by phytoplankton. Journal of Phycology, **44,** 1171–1187.

Flynn, K.J., Fasham, M.J.R. and Hipkin, C.R. (1997). Modelling the interaction between ammonium and nitrate uptake in marine phytoplankton. Philosophical Transactions of the Royal Society B, **352,** 1625-1645.

Ford, A. (1999). Modeling the environment: an introduction to system dynamics modeling of environmental systems, Island press.

Forrester, J.W. (2007). System dynamics a personal view of the first fifty years. System Dynamics Review, **23(2-3),** 345-358.

Gelda, R.K. and Effler, S.W. (2007). Testing and application of a two-dimensional hydrothermal model for a water supply reservoir: implication of sedimentation. Journal of Environmental Engineering Science, **6,** 73-84.

Glibert, P.M. and Burkholder, J. A. M. (2011). Harmful algal blooms and eutrophication:"strategies" for nutrient uptake and growth outside the Redfield comfort zone. Chinese Journal of Oceanology and Limnology, 29(4), 724-738.

Glibert, P.M., Allen, J.I., Bouwman, L., Brown, C., Flynn, K.J., Lewitus, A. and Madden, C. (2010). Modeling of HABs and eutrophication: status, advances, challenges. Journal of Marine Systems, **83,** 262-275.

Glibert, P.M., Anderson, D. A., Gentien, P., Granéli, E. and Sellner, K.G. (2005). The global, complex phenomena of harmful algal blooms. Oceanography, **18(2),** 136-147.

Goldman, JC. (1986). On phytoplankton growth rates and particulate C:N:P. Limnol Oceanogr, **31,** 1358–1363.

Grégoire, M. and Friedrich, J. (2004). Nitrogen budget of the north-western black sea shelf as inferred from modeling studies and in-situ benthic measurements. Marine Ecology Progress Series, **270,** 15–39.

Grégoire, M. and Soetaert, K. (2010). Carbon, nitrogen, oxygen and sulfide budgets in the Black Sea: a biogeochemical model of the whole water column coupling the oxic and anoxic parts. Ecological Modelling, **221(19),** 2287-2301.

Gregoire, M., Raick, C. and Soetaert, K. (2008). Numerical modeling of the deep black sea ecosystem functioning during the late 1980s (eutrophication phase). Progress in Oceanography, **76,** 286–333.

Holling, C.S. (1978). Adaptive environmental assessment and management. Reprinted by Blackburn Press in 2005, Wiley,London.

Ishizaka, J., Kitaura, Y., Touke, Y., Sasaki, H., Tanaka, A., Murakami, H., Suzuki, T., Matsuoka, K. and Nakata, H. (2006). Satellite detection of red tide in Ariake Sound, 1998–2001. Journal of Oceanography, **62,** 37–45.

Jonge, V. N. de, Elliott, M. and Orive, E. (2002). Causes, historical development, effects and future challenges of a common environmental problem: eutrophication. Hydrobiologia, 475/476, 1–19.

Joseph, L. and Villareal, T.A. (1998). Nitrate reductase activity as a measure of nitrogen incorporation in Rhizosolenia formosa (H. Peragallo): internal nitrate and dial effects. Journal of Experimental Marine Biology and Ecology, **229,** 159-176.

Kuo, J. T., Hsieh, C. D., Chiu, S. K. and Hsieh, P. H. (2004, January). Optimal best management practices (BMPs) Placement Strategies- Application to Fei-Tsui Reservoir Watershed in Taiwan. Proceedings of World Waterand Environmental Resources Congress, Salt Lake City, Utah,U. S. A.

Kuo, J.T., Hsieh, M.H., Lung, W.S. and She, N. (2007). Using artificial neural network for reservoir eutrophication prediction. Ecological modeling, **200,** 171–177.

Lancelot, C., Hannon, E., Becquevort, S., Veth, C. and de Baar, H. J. W. (2000). Modeling phytoplankton blooms and carbon export production in the Southern Ocean: dominant controls by light and iron in the Atlantic sector in Austral spring 1992. Deep Sea Research Part I: Oceanographic Research, **47,** 1621–1662.

Laws, E. A. and Chalup, M. S. (1990). A microalgal growth model. Limnology and oceanography, **35(3),** 597-608.

Li, Y., Waite, A.M., Gal, G. and Hipsey, M.R. (2013). An analysis of the relationship between phytoplankton internal stoichiometry and water column N: P ratios in a dynamic lake environment. Ecological Modelling, **252,** 196-213.

Mitra, A. and Flynn, K.J. (2010). Modelling mixotrophy in harmful algal blooms: More or less the sum of the parts? Journal of Marine Systems, **83,** 158-169.

Monod, J. (1949). The growth of bacterial cultures. Annual Review of Microbiology, **3,** 371-394.

Nash, J. E. and Sutcliffe J. V. (1970). River flow forecasting through conceptual models part I. Journal of Hydrology, **10 (3),** 282–290.

Nixon, S. W. (1995). Coastal marine eutrophication: a definition, social causes, and future concerns. Ophelia, **41(1),** 199-219.

O'Neil, J., Davis, T.W., Burford, M.A. and Gobler, C.J. (2012). The rise of harmful cyanobacteria blooms: the potential roles of eutrophication and climate change. Harmful Algae, **14,** 313-334.

O'Brien, WJ. (1974). The dynamics of nutrient limitation of phytoplankton algae: a model reconsidered. Ecology, **55,**135-141.

Özkundakci, D., Hamilton, D.P. and Trolle, D. (2011). Modelling the response of a highly eutrophic lake to reductions in external and internal nutrient loading. New Zealand Journal of Marine and Freshwater Research, **45(2),** 165-185.

Ramin, M., Perhar, G., Shimoda, Y. and Arhonditsis, G.B. (2012). Examination of the effects of nutrient regeneration mechanisms on plankton dynamics using aquatic biogeochemical modeling. Ecological Modelling, **240,** 139-155.

Ruley, J.E. and Rusch, K.A. (2004). Development of a simplified phosphorus management model for a shallow, subtropical, urban hypereutrophic lake, Ecological Engineering, **22,** 77–98.

Shirmohammadi, A., Chaubey, I., Harmel, R. D., Bosch, D. D., Muñoz-Carpena, R., Sexton, A., Arabi, M., Wolfe, M. L. and Frankenberger, J. (2006). Uncertainty in TMDL models, Transactions of the ASAE, **49(4),** 1033-1049.

Shuter, B. (1979). A model of physiological adaptation in unicellular algae. Journal of Theoretical Biology, **78,** 519-552.

Simonovic, S.P. and Fahmy, H. (1999). A new modeling approach for water resources policy analysis. Water Resources Research, **35 (1),** 295-304.

Simonovic, S.P. (2000). Tools for water management: one view of the future. Water International, **25(1),** 76–88.

Simonovic, S.P. (2009). Managing water resources: methods and tools for a systems approach. United Nations Educational, Routledge.

Sterman, J. D. (2000). Business dynamics; system thinking and modeling for a complex world. Irwin McGraw-Hill Publication.

Tidwell, V.C., Passell, H.D., Conrad, S.H. and Thomas, R.P. (2004). System dynamics modeling for community-based water planning, application to the Middle Rio Grande. Aquatic Sciences, **66,** 357–372.

Van Engeland, T., Soetaert, K., Knuijt, A., Laane, R. and Middelburg, JJ. (2010). Dissolved organic nitrogen dynamics in the North Sea: a time series analysis (1995–2005). Estuarine, Coastal and Shelf Science, **89(1),** 31-42.

Vezjak. M., Savsek. T. and Stuhler. E. A. (1998). System dynamics of eutrophication process in Lakes. European Journal of Operational Research, **109,** 442-451.